Environmental Earth Sciences

EVOLUTION OF THE POLLUTION IN THE PIEDRAS RIVER NATURAL SITE (GULF OF CADIZ, SOUTHERN SPAIN) DURING THE HOLOCENE
--Manuscript Draft--

Manuscript Number:	ENGE-D-15-01539R1
Full Title:	EVOLUTION OF THE POLLUTION IN THE PIEDRAS RIVER NATURAL SITE (GULF OF CADIZ, SOUTHERN SPAIN) DURING THE HOLOCENE
Article Type:	Original Manuscript
Corresponding Author:	Javier Lario, Ph.D. Universidad Nacional de Educacion a Distancia Madrid, SPAIN
Corresponding Author Secondary Information:	
Corresponding Author's Institution:	Universidad Nacional de Educacion a Distancia
Corresponding Author's Secondary Institution:	
First Author:	Javier Lario, Ph.D.
First Author Secondary Information:	
Order of Authors:	Javier Lario, Ph.D.
	Jacinto Alonso-Azcárate, Ph.D.
	Christopher Spencer, Ph.D.
	Cari Zazo, Ph.D.
	Jose L Goy, Ph.D.
	Ana Cabero, Ph.D.
	Cristino J Dabrio, Ph.D.
	Francisco Borja, Ph.D.
	Cesar Borja, Ph.D.
	Jorge Civis, Ph.D.
	Manuel Garcia-Rodriguez, Ph.D.
Order of Authors Secondary Information:	
Funding Information:	Ministerio de Economía y Competitividad (ES) (CGL2013-42847-R) — Dr. Javier Lario
	Ministerio de Economía y Competitividad (ES) (CGL2012-33430) — Dr. Cari Zazo
	University of Bristol (GB) — Dr. Christopher Spencer

Abstract:	The Piedras River marshland and El Rompido spit bar is a Natural Site in close proximity to two of the most polluted rivers in the world: the Tinto and Odiel Rivers. The aim of this study is to determine the degree of contamination of this Natural Site using a variety of pollution indices. At this site the Holocene infilling sequence is recorded and applied to a study of the pollution history and the possible impacts of human activity. The depositional history of the Piedras River estuary during the Holocene recorded open marine conditions at ca. 6500 calBP when sea-level was at its Holocene maximum. To study the pollution of the estuary during the Holocene, catchment background geochemistry was established using samples that pre-date human activity (agriculture and mining). Additionally, the sedimentary environment

was reconstructed throughout the Holocene, comparison of pollution levels is interpreted to be more reliable if the sedimentary environment has remained similar throughout the depositional record. Results show that, despite being located nearby very polluted estuaries, the Piedras River marshland contains unpolluted sediments mainly because of the small catchment area relative to that of neighbouring more polluted rivers, and thus not been affected by human activity such as mining.

EVOLUTION OF THE POLLUTION IN THE PIEDRAS RIVER NATURAL SITE (GULF OF CADIZ, SOUTHERN SPAIN) DURING THE HOLOCENE

J. Lario (1), J. Alonso-Azcárate (2), C. Spencer (3), C. Zazo (4), J.L. Goy (5), A. Cabero (1), C.J. Dabrio (6), F. Borja (7), C. Borja (8), J. Civis (9), M. García-Ródriguez (1)

(1) Facultad de Ciencias, Universidad Nacional de Educación a Distancia (UNED), 28040-Madrid, Spain.*

(2) Facultad de Ciencias del Medio Ambiente, Universidad de Castilla la Mancha, 45071-Toledo, Spain.

(3) Faculty of Environment and Technology, University of the West England, Bristol BS16 1QY, United Kingdom.

(4) Departamento de Geología, Museo Nacional de Ciencias Naturales-CSIC, 28006-Madrid, Spain.

(5) Departamento de Geología, Facultad de Ciencias, Universidad de Salamanca, 37008-Salamanca, Spain.

(6) Departamento de Estratigrafía & IGE (CSIC), Universidad Complutense, 28040-Madrid, Spain.

(7) Área de Geografía Física, Facultad de Humanidades, Universidad de Huelva, 21007-Huelva, Spain.

(8) Facultad de Geografía e Historia, Universidad de Sevilla, 41004-Sevilla, Spain.

(9) Instituto Geológico y Minero de España-IGME, 28003-Madrid, Spain.

* corresponding author: javier.lario@ccia.uned.es

Abstract

The Piedras River marshland and El Rompido spit bar is a Natural Site in close proximity to two of the most polluted rivers in the world: the Tinto and Odiel Rivers. The aim of this study is to determine the degree of contamination of this Natural Site using a variety of pollution indices. At this site the Holocene infilling sequence is recorded and applied to a study of the pollution history and the possible impacts of human activity. The depositional history of the Piedras River estuary during the Holocene recorded open marine conditions at ca. 6500 calBP when sea-level was at its Holocene maximum. To study the pollution of the estuary during the Holocene, catchment background geochemistry was established using samples that pre-date human activity (agriculture and mining). Additionally, the sedimentary environment was reconstructed throughout the Holocene; comparison of pollution levels is interpreted to be more reliable if the sedimentary environment has remained similar throughout the depositional record. Results show that, despite being located nearby very polluted estuaries, the Piedras River marshland contains unpolluted sediments mainly because of the small catchment area relative to that of

1

32 neighbouring more polluted rivers, and thus has not been affected by human activity such as

33 mining.

34

35 Keywords: Holocene sediments; Metal pollution; Heavy metals; Contamination factor;

36 Enrichment factor; Geo-accumulation index

37

1. Introduction

39 The Piedras River marshland and El Rompido spit bar Natural Site is located in Huelva

40 Province, SW Spain (Figure 1) and extends for 2,530 ha. The area was declared a Natural Site

41 in 1989 and also a Special Area of Conservation of Wild Birds in 2002. The area has been

42 proposed as a European Site of Community Importance. This Natural Site is located at the

43 mouth of the Piedras River containing a tidal marshland protected from the Atlantic Ocean by a

44 ~12 km long spit bar. This estuary is located between the Guadiana River to the west and the

45 Tinto and Odiel Rivers to the east. These rivers drain the Iberian Pyrite Belt, the largest

46 repository of volcanogenic massive sulphide deposits in the world, and as a result of mining

47 within the catchment areas both rivers have high levels of pollution (Borrego et al. 2004;

48 Delgado et al. 2009).

49 The geology of the drainage basin is represented in Figure 2. To the north, the Hercinian

50 deposits are represented by Carboniferous dolomites, dolomitic limestone's and marls. Miocene

51 deposits consist mainly of calcarenites and yellow silts while Pliocene deposits consist of grey-

52 yellow sands and silty sand. The Quaternary deposits are represented by river terraces in the

53 upper areas and eolian and marsh deposits in the lower areas.

54 The special geological characteristics of this area have led to research on the trace metals

55 present in the sediments of the estuaries located in this area in order to evaluate the degree of

56 contamination (Ruiz 2001; Santos Bermejo et al. 2003; Borrego et al. 2004; Lozano-Soría et al.

57 2005; Sainz and Ruiz 2006; Ruiz et al. 2009; Delgado et al. 2010; Carretero et al. 2011). Most

58 of this research has been focussed on the Guadiana and Tinto-Odiel estuaries, while research

59 in the Piedras River estuary has been less extensive and only using surface samples. Sainz

2

60 and Ruiz (2006) studied the influence of the very polluted Tinto-Odiel River and concluded that

61 the littoral fringe extending up to 50 Km is classified as moderately to strongly polluted. Due to

62 dominant longshore currents along this coast much of this pollution is transported to the east,

63 some pollution is though transported to the west, reaching the mouth of the Piedras River

64 estuary. Due to the high interest in this area as a Natural Site, the major objective of this study

65 is to evaluate the potential heavy-metal pollution in surface and deep sediments of the

66 marshland through the last 7000 yrs. This is the first time core samples have been recovered in

67 order to study the pollution history of the area enabling the determination of the local

68 background values for the heavy metals in the Piedras River estuary. In addition an attempt is

69 made here to evaluate whether the anthropogenic activity resulting in the pollution recorded in

70 the sedimentary record of the two adjacent river estuaries is present in the sedimentary record

71 of the Piedras River estuary.

72 To study the heavy metal pollution in estuarine sediments indices such as contamination factor

73 (CF), geoacumulation index (I_{geo}) and enrichment factor (EF) have been used in other coastal

74 areas (Rubio et al. 2000; Srinivasa Reddy et al. 2004; Chen et al. 2007; Praveenna et al. 2008;

75 Darasam et al. 2011; Feng et al. 2011) and are still used to assess contamination in soils, river

76 environments, estuaries, lakes, reservoirs or urban sediments (Kumar et al. 2013, Zahra et al.

77 2014, Diop et al. 2015, Elkady et al. 2015, El-Sayed et al. 2015, Palma et al., 2015, Rivera et al.

78 2015, Ma et al. 2016). In order to assess sediment contamination at this location the indices

79 cited above have been calculated with comparisons made between sediments deposited pre

80 and post anthropogenic activity in the area. These indices have been correlated with other

81 factors such as particle size and total organic carbon (TOC) values of the sediments.

82

83 **2. Methodology**

84 2.1. Sampling and analyses

85 A total of eighteen manual gouge and percussion boreholes were completed in the study area.

86 For this study three percussion cores were selected that included a full record of the Holocene

87 infilling sequence (cores RP-11, RP-15 and RP-16, Figure 1). These cores were sampled into

88   plastic pipes and stored in a fridge at -4ºC, cores were then cut longitudinally and sampled at

89   intervals of 20 cm resulting in a total of 91 samples. Contamination was avoided by discarding

90   the outer layer of each core section. Dates from cores were established by Lario et al. (2009)

91   through radiocarbon dating. The ages and sedimentation rates agree with data available for

92   others estuaries in the Gulf of Cadiz (Lario et al. 2002).

93   The bulk content of Cr, Cu, Ni, Pb and Zn present in the sediments was studied as they are the

94   main heavy metals present in the area (Leblanc et al. 2000; Ruiz et al. 2008) in addition they

95   are the trace metals typically determined in heavy metal contamination studies (Kanellopoulos

96   et al. 2006, Feng et al. 2011). To determine the total concentration of metals in the sediment

97   samples, 0.5g of the <63µm fraction (dry weight) obtained by dry sieving was used. The <63µm

98   fraction was utilised as the content of heavy metals is normally accumulated in the fine fractions

99   associated to clay minerals and oxides (Soares et al. 1999, Fan et al. 2002, Cuong and Obbard

100   2006). The samples were digested with a mixture of acids (9ml of concentrated HNO_3 + 3ml of

101   concentrated HCl) in Teflon® PTFE (polytetrafluoroethylene) beakers in a microwave unit (CEM

102   MARS 5, Matthews, USA), according to EPA 3051A method (USEPA, 1996). Dissolved

103   samples were then diluted to 40ml with milli-Q water. Following digestion, the heavy metal

104   concentration in the sample solutions and reagent blanks was measured by ICP-AES in a

105   Thermo iCAP 6500 spectrometer and by ICP-MS in a Thermo X-Series II spectrometer (Thermo

106   Electron, Cambridge, UK). All reagent blanks and matrix interference were monitored

107   throughout the analyses, and were below the instrument detection limit. The analytical method

108   was assessed by using the 2711 Standard Reference Material (Montana Soil, from LGC

109   Promochem, Barcelona, Spain) with an agreement of 93.3–107.7% between the certified values

110   and the concentrations obtained by this study. Al and Fe were determined by X-ray

111   fluorescence spectrometry, using a Phillips Spectrometer PW 1410/20 with a PW 1730

112   generator.

113   Particle size distribution was analysed by laser diffraction using a Coulter® LS 230 and Carbon

114   content (total, organic-TOC- and inorganic-IC) of the sediments was analysed using a

115   Shimadzu® TOC-VCSH analyser.

4

116

2.2. Use of pollution Indices

The metal content in sediments is the result of an addition of metals originating from natural sources and anthropogenic activity. It is estimated that the contribution of metals incorporated in sediments as a result of human causes is higher than the contribution from natural processes (Nriagu and Pacyna 1988). In a long term study such as this across the Holocene the identification of phases of raised metal concentration in sediments would typically be related with significant changes in human activities in the catchment area. Establishing the pollution history of the estuary and thus human activity in the catchment area is thus value to archaeological study of the area.

In this study, the possible sediment contamination was assessed using various pollution indices, including contamination factor and degree of contamination, index of geoaccumulation and normalized enrichment factor, these are outlined below.

129

Contamination Factor (CF)

The assessment of sediment contamination has been carried out using the contamination factor (CF) and contamination degree (CD). The approach suggested by Hakanson (1980) is applied which enables an assessment of sediment contamination through using pre-industrial levels as a reference of the background concentrations enabling comparison with post-industrial sediments.

Calculation will be simplified as:

CF=Cm/Cb

where Cm is the mean content of an individual metal in the sample and Cb is the pre-industrial concentration of an individual metal (background concentration). This should then identify a direct relationship between the concentration of a specific metal and how this corresponds to the background level.

Hakanson (1980) define four categories of contamination factor (CF)

CF < 1   low contamination factor

144 1<CF<3   moderate contamination factor

145 3<CF<6   considerable contamination factor

146 CF > 6   very high contamination factor

147 The contamination factor described above is a single element index. The sum of contamination

148 factors for all elements examined represents the contamination degree (CD) of the environment

149 and four classes are recognized (Hakanson 1980)

150 CD < 8   low degree of contamination

151 8 < CD < 16   moderate degree of contamination

152 16 < CD < 32 considerable degree of contamination

153 CD >32   very high degree of contamination

154

Geo-accumulation index (I_{geo})

156 The geoaccumulation index (I_{geo}) has been used since the late 1960s, and has been widely

157 employed in trace metal studies. Müller (1969) first used this index in basal sediments but it has

158 also been used largely to evaluate contamination in soils (Loska et al. 2003; 2004; Yaqin et al.

159 2008, Rivera et al., 2015), rivers (Ma et al., 2016), lakes (Zahra et al., 2014, Elkady et al.,

160 2015), beaches (Diop et al., 2015), mangroves (Praveena et al. 2008), *Ria* type embayment

161 coasts (Rubio et al. 2000) or even harbours (Chen et al. 2007) and reservoirs (Goher et al.,

162 2013, Palma et al., 2015). The *Igeo* enables the assessment of contamination by comparing

163 current and pre-industrial concentrations, although it is not always easy to reach pre-industrial

164 sediment layers (Yaqin et al., 2008). In this study, the I_{geo} for selected sediments was calculated

165 using

166 $I_{geo} = log_2 (Cm/1.5\ Cb)$

167 where *Cm* is the measured concentration of the element in the sediment and *Cb* is the

168 geochemical background value. The constant 1.5 is used to analyse natural fluctuations in the

169 content of a given substance in the environment and to detect very small anthropogenic

170 influences. It is also a factor used for lithological variations of trace metals.

171 The geoaccumulation index consists of seven grades or classes (Müller 1979; 1981)

172　　$I_{geo} < 0$　　　　I_{geo} Class = 0　practically uncontaminated

173　　$0 < I_{geo} < 1$　　　I_{geo} Class = 1　uncontaminated to moderate contaminated

174　　$1 < I_{geo} < 2$　　　I_{geo} Class = 2　moderate contaminated

175　　$2 < I_{geo} < 3$　　　I_{geo} Class = 3　moderate to strong contaminated

176　　$3 < I_{geo} < 4$　　　I_{geo} Class = 4　strong contaminated

177　　$4 < I_{geo} < 5$　　　I_{geo} Class = 5　strong to very strong contaminated

178　　$I_{geo} > 5$　　　　I_{geo} Class = 6　very strong contaminated

179

Enrichment Factor (EF)

181　The use of EF has been very widely applied as a means of identifying and quantifying the

182　anthropogenic origin of certain elements since the 1970s (Chester and Stoner 1973; Duce et al.

183　1975), it is also a convenient measure of geochemical trends and is used for making

184　comparisons between areas (Sinex and Helz 1981) and it is still widely used (e.g. Puig et al.

185　1999; Rubio et al. 2000; Karageorgis and Hatzianestis 2003; Loksa et al. 2003; 2004; Selvaraj

186　et al. 2004; Vazquez and Sharma 2004; Kanellopoulos et al. 2006; Radakovitch et al. 2008).

187　The extent of metal contamination compared to the background of the catchment area was

188　assessed using the enrichment factor (EF) (Woitke et al. 2003; Selvaraj et al. 2004). The EF

189　was also based on the standardization of a tested element against a reference one. A reference

190　element is the one characterized by low occurrence variability such as Sc, Mn, Ti, Al and Fe

191　(Pacyna and Winchester 1990; Quevauviller et al. 1989; Schiff and Weisberg 1999; Reimann

192　and De Caritat 2000; Sutherland 2000).

193　Some authors used Al to normalize the metals in sediments since it represents the

194　aluminasilicates, the predominant content of coastal sediments (Chen et al. 2007, Delgado et al.

195　2010) but other observations support that either Al or Fe can be used for metal normalization if

196　there is a significant correlation between them (Feng et al. 2011). Lozano-Soria et al. (2005)

197　found a high positive correlation between Al and Fe in Piedras River sediments and thus in this

198　study Al and Fe were used as reference elements for metal normalization.

199 The enrichment factor was calculated using the formula based on the equation suggested by

200 Buat-Menard and Chesselet (1979):

201 $EF = [Cm)/Cr)]/[Cmb/Crb]$

202 where, Cm is the content of the metal in sample, Cr is the content of the reference element in

203 the sample, Cmb is the content of the metal in the background sample and Crb is the content

204 of reference element in the background sample.

205 In this case

206 $EF_{Al} = [Cm)/C_{Al})]/[Cmb/C_{Al}b]$

207 $EF_{Fe} = [Cm)/C_{Fe})]/[Cmb/C_{Fe}b]$

208 Five contamination categories are recognized on the basis of the enrichment factor (Sutherland,

209 2000)

210 EF<2   deficiency to mineral enrichment

211 2<EF<5   moderate enrichment

212 5<EF<20   significant enrichment

213 20<EF<40   very high enrichment

214 EF>40   extremely high enrichment

215

216 2.3. Analysis of results

217 A contrast independence test was carried out with the aim of determining whether significant

218 relationships exist between variables. In addition a study of the data distribution was completed

219 to establish the tests (parametric or non-parametric) that could be applied. A Kolmogorov-

220 Smirnov (K-S) test was used to check the normality of the variables. Whilst Pearson Correlation

221 Coefficient (R) and Spearman Correlation Coefficient (rs) tests were used for Normal and Non-

222 Normal distribution, respectively. *SPSS* software was used for the calculations. This

223 methodological approach has been applied in other geoacummulation indexes studies (Rubio et

224 al., 2000, Diop et al., 2015).

225

226 **3. Results and Discussion**

3.1. Sedimentary framework

From the cores studied it is possible to interpret the Late Pleistocene and Holocene evolution of the Piedras River estuary, and thus the pollution during this period. The river is incised into coarse-grained Quaternary sediments deposited during the last major lowstand ca. 18 ka, when sea level was ~120 m lower and the coastline lay 14 km seawards from the present (Dabrio et al., 2000). Some studies of estuaries and lagoons on the coast of south-western Iberia have shown that the post-glacial transgression reached larger valleys such as the Tagus (Vis et al., 2008), Guadiana (Boski et al.,2002,2008; Delgado et al., 2012), Tinto-Odiel (Dabrio et al., 1999, 2000) and Guadalquivir (Dabrio et al.,1999, 2000) estuaries between 13,000 calBP and 10,000 calBP. Smaller valleys were only inundated when sea level reached its post-glacial maximum at about 7500-6500 calBP (Dabrio et al., 1999; Freitas et al., 2002; Schneider et al., 2010). In the Piedras River estuary the sediments underlying the Holocene estuary sequence are Miocene Pliocene (Figure 2). According to the interpretation (Lario et al., 2009) and the radiocarbon data obtained (Figure 2) the transgressed estuary basins changed from brackish to more open marine conditions as the sea rose until ca. 6500 calBP, when it reached the maximum height and the sandy estuarine barriers ceased to prograde toward the muddy central basins. Then, as it has been observed in other estuaries from the Gulf of Cadiz, rates of sedimentation and the eustatic sea-level rise decreased significantly, and the estuarine infilling was dominated by lateral progradation (Lario et al., 2002). At ca. 4000 calBP the fluvial input exceeded the rate of sea-level rise, causing partial emergence of tidal flats in the mostly filled estuarine basin. Dominance of coastal progradation upon vertical accretion at ca. 2800-2200 calBP favoured the spreading out of tidal flats and sandy barriers. Some high energy (erosional) episodes have been recorded in the upper sequence as have been interpreted in others areas of the Gulf of Cadiz (Lario et al. 2010, 2011). Also, the development of the El Rompido spit barrier during the last two centuries has partially enclosed the estuary for the first time during the Holocene.

3.2. Selecting geochemical background values

254   Through all the indices calculated, the *Cb* parameter in the equations represents the

255   geochemical background value. The equations indicate that the index will be affected by the

256   content of the samples and the geochemical background values.

257   Some authors have proposed as background reference the world average shale (Rubio et al.

258   2000) or the Earth's crust (Loska et al. 2003, 2004). However, these levels tend to be very

259   general and may distort the results. Rubio et al. (2000) recommended the use of regional

260   background values. While the geochemical background values are constant, the levels of

261   contamination vary with time and space.

262   In this study, in order to evaluate the possible contamination of the area during the last 7000 yr,

263   samples have been selected as background value samples that relate to 'natural' conditions,

264   pre-dating the human activity. According to archaeological data, the extraction of minerals from

265   the catchment area dates back to the age of the Iberians and Tartessos, some 5000 years ago

266   (Davis et al. 2000; Leblanc et al. 2000; Nocete et al. 2005). Samples of that age also represent

267   a significant point in the depositional history of the Piedras River estuary at ca. 6500 calBP,

268   when open marine were recorded representing the Holocene sea-level maximum. Thus,

269   samples corresponding to this age are appropriate to be used as a background level because

270   they represent the beginning of infilling of the estuary after the maximum Holocene

271   transgression and are unpolluted by anthropogenic activity. Importantly the environmental

272   reconstruction identifies that the sedimentary environment has remained relatively consistent

273   since ca. 6500 calBP, as recorded in other nearby estuaries (Lario et al. 2002), enabling reliable

274   comparison of contamination levels through this time period.

275   Therefore, to estimate the background values, five samples from core RP-15 dated ca.6500

276   calBP were analysed and the mean values calculated. The values for the average background

277   in the Piedras River estuary produced from this analysis were Cr: 45.8 mg/kg, Cu: 16.1 mg/kg,

278   Ni: 27.2 mg/kg, Pb: 13.7 mg/kg and Zn: 62.2 mg/kg (Table 1).

279   Different background values have been calculated for the different estuaries in the south-

280   western Spanish coast (Ruiz et al. 1998, Delgado et al. 2008; Carretero et al. 2011; Delgado et

281   al. 2012; Table 1). All of them are based on samples of Holocene age except the one calculated

282 for the Tinto-Odiel estuary in which samples of Neogene and Holocene age have been used.

283 The background values for the Tinto-Odiel estuary are slightly lower than for the other three

284 estuaries, probably reflecting the larger time-span of samples used for the calculation. The other

285 three estuaries show very similar background values, particularly the Doñana and Piedras River

286 estuaries. Only the value of Cr for the Doñana estuary is significantly higher than in the other

287 three, indicating the necessity of calculating the background values for each studied area, as

288 local geological variations can lead to variations in the geochemistry of sediments and thus the

289 background values among areas with similar geology.

290

291 3.3. Contamination Indices

292 A total of 91 samples from the three cores have been analysed in order to evaluate the possible

293 record of pollution through time at the site. Particle size distribution, organic carbon content and

294 metal concentration values are presented in Tables 2, 3 and 4. For the three cores the

295 proportion of the clay fraction in the sample was low, generally under 10%. In cores RP-15 and

296 RP-11 the silt fraction predominated while in RP-16 the sandy dominated. TOC values were not

297 very high ranging between 0 and 1.76%, typically increasing towards the top of the three cores

298 due to the organic carbon decomposition in older sediments (Kanellopoulos et al. 2006). Mean

299 TOC values decreased along the profile towards the more marine locations in the estuary (RP-

300 11>RP-15>RP-16, Figures 1 and 2).

301 For the study of the contamination indices, 14 samples have been selected (Table 5)

302 representing different periods of time through the Holocene from the time of maximum sea-level.

303 The samples represent the estuarine filling sequence and therefore any natural changes (e.g.

304 flooding, increase in erosional rates…) or human induced changes (e.g. minning, farming…)

305 during this time should be recorded. In addition, some older samples (up to ca. 9000 calBP)

306 have been analysed in order to compare the estuarine background values with previous natural

307 values and to detect any previous input of metals to the basin due to alluvial episodes or

308 leaching of metallic deposits.

11

309   Table 6 shows the CF values for the selected samples. All values were in the *low contamination*

310   *factor* or low values *of moderate contamination factor* categories. Therefore, all samples

311   showed a low degree of contamination except for the surface samples, which showed a

312   moderate degree of contamination.

313   The I_{geo} (Table 7) shows the same tendency as the CF index with uncontaminated levels in

314   most samples. I_{geo} values are lower than 1, which classifies the sediments as unpolluted,

315   similar to the values calculated by Ruiz (2001) in surface samples. The enrichment factors (EF_{Al}

316   and EF_{Fe}, Table 8) both showed similar trends and most samples indicate deficiency to mineral

317   enrichment.

318

319   3.4. Statistical Analysis

320   Tables 9, 10, and 11 shows the Pearson correlation matrix for the particle size fractions, TOC

321   and the heavy metals studied. It can be seen that both the grain size and total organic carbon

322   are important factors affecting the metal distribution in the sediments with high correlation

323   factors. Generally there is a strong correlation between the quantity of the fine fractions and

324   trace metal concentrations (Wang and Chen 2000; Huang and Lin 2003) while in this study the

325   TOC values were relatively more important than grain size in controlling the distribution of trace

326   metals in the sediments as it correlates with higher values with all metals than with the clay

327   content. These results demonstrate that organic matter content was a more important factor

328   affecting the trace metal concentrations than the grain size distribution. The Cr, Ni, Pb, Zn and

329   Cu correlate positively for all the sections, which indicate a common geogenic origin for the

330   assemblage.

331   TOC has a positive correlation with clay and silt fractions and negative with the sand fraction

332   (Tables 9, 10 and 11) which indicates that organic matter in the sediments was fine to very fine

333   grained.

334   The study of all the contamination indices clearly shows a consistent trend indicating that the

335   Piedras River estuary sediments display no signs of contamination as a result of human activity

336   during the Holocene. This greatly contrasts with the situation of the adjacent estuaries.

12

337 The Iberian Pyrite Belt (IPB), with over 1,600 million tons of polymetallic massive sulphide

338 deposits originally in place and about 2,500 million tons of mineralization in the stockwork, is

339 one of the most significant metallogenic areas in the world and possibly the largest

340 concentration of sulphides worldwide. Also, the Iberian Pyrite Belt is one of the oldest mining

341 districts in the world with mining activity recorded over the last 5000 years. Mining commenced

342 in the Chalcolithic period (3rd millennium BC) and continued during the Bronze Age and

343 Tartessian civilization. During Roman times industrial mining extracted more than 20 million

344 tons. After the abandonment of the mines in the 4th century BC, the mines were exploited only

345 on a minor scale. In the late nineteenth century the mining was operated by British and French

346 companies, and large-scale, open-pit operations prevailed until the deposits had been

347 essentially depleted about a century later. Due to this activity the Tinto and Odiel Rivers

348 represent an extreme case of acid mine drainage with high concentrations of toxic elements.

349 The many sources of pollution, along with the low buffering capacity of the rocks that form the

350 substrate of the basins of the Tinto and Odiel Rivers, result in high levels of contamination,

351 unparalleled worldwide. (Ruiz 2001; Sainz and Ruiz 2006; Olias and Nieto 2012).

352 In the Doñana estuary relatively polluted sediments (3800-3000 calBP) have been found

353 derived from old mining activities located in its catchment area (Carretero et al. 2011). In the

354 Guadiana estuary Delgado et al. (2012) determined background levels from core sediments

355 unaffected by human activities and determined that the surface elements of the estuary with

356 ages younger than 4500 calBP contain significant levels of contamination associated with the

357 mining activities in the IPB. Firstly the Guadiana Estuary sediments record a general increase in

358 elements such as Co, Cr and Ni in the Copper Age, in the Bronze age and in the Roman period

359 greater increases of heavy metals were recorded. Finally the most recent period of modern

360 mining activities are also recorded in the heavy metal contents of the estuary sediments.

361 The absence of pollution in Piedras River estuary is interpreted as being due to the fact that in

362 the Piedras River catchment area there are no mineral ore deposits and thus no historic mining

363 activity. Sainz and Ruiz (2006) found that the presence of pollution at the mouth of the Piedras

364 River indicates the influence of flow from the Tinto and Odiel Rivers. Absence of this pollution in

365 the estuarine sediments indicate than the inner estuary has not been influenced by discharge
366 from the Tinto and Odiel Rivers during the Holocene and, therefore, the dominant longshore
367 currents in this area have remained the same (towards the east) throughout the Holocene.
368 There is no evidence of the transfer of contaminants between the closed basins by wind or by
369 the sea, and thus sedimentation in the Piedras River is dominated by fluvial input rather than
370 from extra-estuary marine sources.

371 Data obtained in this study supports that of studies of surficial pollution in the Piedras River
372 estuary (Ruiz 2001; Lozano-Soria et al. 2005), that found very low or unpolluted sediment.
373 Furthermore we found that this characteristic extends throughout the last 7000 yr confirming
374 that the area has not been influenced by pollution from human activity during the Holocene.
375 Whilst similarities exist between this study and the previous studies in the region it must be
376 stressed that previous work was limited to surficial samples and used background values from
377 the nearby Tinto-Odiel estuary. Therefore, this study represents the first investigation where the
378 research has included the study of the entire estuarine sequence and has used local
379 geochemical background values in order to evaluate the record of the trace metals in the
380 estuary trough the time.

381

382 **Conclusions**

383 This study evaluated the degree of heavy-metal contamination of the Piedras River Natural Site
384 using a variety of pollution indices. Through analysing sediments derived from deep coring it
385 has been possible to recover the entire Holocene sedimentary sequence of the estuary and for
386 the first time local geochemical background values of uncontaminated sediments has been
387 established.

388 The comparison of background geochemical values from different estuaries in the area reveals
389 the necessity of calculating the background values for an estuary using local data and an
390 adequate time-span. Local geological variations can result in key changes in the geochemistry
391 of sediments producing changes in the background values among areas with similar geology.

14

392 For the first time in the Piedras River estuary this work uses the study of the entire estuarine

393 sequence and local geochemical background data, in order to evaluate the evolution of the

394 trace metals in the estuary trough the time. Pollution indices reveal low or unpolluted sediments,

395 extending through the last 7000 yr, and confirming that the area has not been influenced by

396 pollution from human activity during the Holocene. The results presented here agree with

397 previous work on this estuary that was limited to surficial samples, and using regional

398 background values (from the nearby Tinto-Odiel estuary, Ruiz 2001; Lozano-Soria et al. 2005).

399 Results show that all of the pollution indices calculated dismiss any trace of heavy-metal

400 pollution through the last 7000 years and therefore there is no evidence of any minning activity

401 in this catchment area. The heavy-metal concentrations are of geogenic origin and appear to be

402 linked to the amount of fine grained organic matter in the sediments rather to clay fraction. The

403 results also indicate that the estuary has not been influenced by extra-estuary pollution sources

404 from the nearby polluted Guadalquivir Rivers, Guadiana River or Tinto and Odiel Rivers. It can

405 also be inferred that the dominant longshore currents in this area have remained the same

406 during the Holocene and that sedimentation in the Piedras River estuary is dominated by fluvial

407 input rather that extra-estuary marine sources. This study provides new pollution data and detail

408 of estuary evolution during Holocene; such details are relevant for the preservation of this

409 Natural Site and Special Area of Conservation of Wild Birds.

410

414

References:

416 Buat-Menard, P., Chesselet, R. 1979. Variable influence of the atmospheric flux on the trace

417 metal chemistry of oceanic suspended matter. Earth Planet. Sci. Lett. 42: 398-411.

15

418   Borrego, J.; López-Gonzalez, N.; Carro, B. 2004. Geochemical signature as paleoenvironmental

419   markers in Holocene sediments of the Tinto River estuary (Southwestern Spain).

420   Estuarine, Coastal and Shelf Science 61: 631-641.

421   Boski, T., Moura, D., Veiga-Pires, C., Camacho ,S., Duarte, D., Scott, D.B., Fernandes, S.G.

422   2002. Postglacial sea-level rise and sedimentary response in the Guadiana Estuary,

423   Portugal/Spain border. Sedimentary Geology 150: 103-122.

424   Boski, T., Camacho, S., Moura, D., Fletcher, W., Wilamowski, A., Veiga-Pires, C., Correia, V.,

425   ,Loureiro, C., Santana,P. 2008. Chronology of the sedimentary processes during the

426   postglacial sea level rise in two estuaries of the Algarve coast, Southern Portugal.

427   Estuarine, Coastal and Shelf Sciences 77: 230-244.

428   Carretero, M.I., Pozo, M., Ruiz, F., Rodríguez-Vidal, J., Cáceres, L.M., Abad, M., Muñoz, J.M.,

429   Gómez, F., Campos, J.M., González-Regalado, M.L., Olías, M. 2011. Trace elements in

430   Holocene sediments of the southern Doñana National Park (SW Spain): historical

431   pollution and applications. Environ. Earth Sci. 64: 1215-1223.

432   Chen, C., Kao, C. Chen, CF., Dong, C. 2007. Distribution and accumulation of heavy metals in

433   the sediments of Kaohsiung Harbor, Taiwan. Chemosphere 66: 1431-1440.

434   Chester, R., Stoner, J.H. 1973. Pb in particulates from lower atmosphere of the eastern Atlantic.

435   Nature 245: 27-28.

436   Cuong D.T., Obbard, J.P. 2006. Metal speciation in coastal marine sediments from Singapore

437   using a modified BCR-sequential extraction procedure. Appl. Geochem. 21: 1335-1346.

438   Dabrio, C.J.; Zazo, C.; Lario, J.; Goy, J.L.; Sierro, F.J.; Borja, F.; González, J.A.; Flores, J.A.

439   1999. Sequence stratigraphy of Holocene incised-valley fills and coastal evolution in the

440   Gulf of Cadiz (southern Spain). Geologie en Minjbow 77: 263-281.

441   Dabrio, C.J.; Zazo, C.; Goy, J.L.; Sierro, F.; Borja, F.; Lario, J.; González, J.A.; Flores, J.A.

442   2000. Depositional history of estuarine infill during the Late Pleistocene-Holocene

443   postglacial transgression. Marine Geology, 162: 381-404.

16

444 Dasaram, B., Satyanarayanan, M., Sudarshan, V., Keshav Krishna, A. 2011. Assessment of

445 Soil Contamination in Patancheru Industrial Area, Hyderabad, Andhra Pradesh, India.

446 Research Journal of Environmental and Earth Sciences 3: 214-220.

447 Davis, R.A., Welty, A.T., Borrego, J., Morales, J.A., Pendón, J.G., Ryan, J.G. 2000. Rio Tinto

448 estuary (Spain): 5000 years of pollution. Environmental Geology 39: 1107-1116.

449 Delgado, J., Nieto, J.M., Boski, T., Alabardeiro, L. 2008. Determinación de los valores de fondo

450 regional en sedimentos Holocenos del estuario del río Guadiana (SW de España).

451 Geogaceta 44: 235-238.

452 Delgado, J., Sarmiento, A., Condesso de Melo, M., Nieto, J. 2009. Environmental impact of

453 mining activities in the southern Sector of the Guadiana basin (SW of the Iberian

454 Peninsula). Water, Air, and Soil Pollution 199: 323-341.

455 Delgado, J., Nieto, J.M., Boski, T. 2010. Analysis of the spatial variation of heavy metals in the

456 Guadiana Estuary sediments (SW Iberian Peninsula) based on GIS mapping techniques.

457 Estuarine. Coastal and Shelf Science 88: 71-83.

458 Delgado, J., Boski, T., Nieto, J.M., Pereira, L., Moura, D., Gomes, A., Sousa, C., García-

459 Tenorio, R. 2012. Sea-level rise and anthropogenic activities recorded in the late

460 Pleistocene/Holocene sedimentary infill of the Guadiana Estuary (SW Iberia). Quarter.

461 Sci. Rev. 33: 121-141.

462 Diop, C., Dewaelé, D., Cazier, F., Diouf, A., Ouddane, B. 2015. Assessment of trace metals

463 contamination level, bioavailability and toxicity in sediments from Dakar coast and Saint

464 Louis estuary in Senegal, West Africa. Chemosphere 138: 980-987.

465 Duce, R. A., Hoffmann, G. L., Zoller, W. H. 1975. Atmospheric trace metals at remote northern

466 and southern hemisphere sites: Pollution or natural?. Science, 187: 59-61.

467 Elkady, A.A., Sweet, S.T., Wade, T.L., Klein, A.G. 2015. Distribution and assessment of heavy

468 metals in the aquatic environment of Lake Manzala, Egypt. Ecological Indicators 58:

469 445-457.

470 El-Sayed, S.A., Moussa, E.M.M., El-Sabagh, M.E.I. 2015. Evaluation of heavy metal content in

471 Qaroun Lake, El-Fayoum, Egypt. Part I: Bottom sediments. Journal of Radiation

472 Research and Applied Sciences 8: 276-285.

473 Fan,W.H., Wang,W.X., Chen, J.S., LI,X.D., Yen, Y.F. 2002. Cu, Ni, and Pb speciation in surface

474 sediments from a contaminated bay of northern China. Mar. Pollu. Bull. 44: 820-826.

475 Feng, H., Jiang, H., Gao, W., Weinstein, M.P., Zhang, Q., Zhang, W., Yu, L., Yuan, D., Tao, J.

476 2011. Metal contamination in sediments of the western Bohai Bay and adjacent

477 estuaries, China. J. Environ. Manage. 92: 1185-1197.

478 Freitas, M.C., Andrade, C., Cruces, A., 2002. The geological record of environmental changes

479 in southwestern Portuguese coastal lagoons since the Lateglacial. Quaternary

480 International 93-94: 161-170.

481 Goher, M.E., Farhat, H.I., Abdo, M.H., Salem, S.G., 2014. Metal pollution assessment in the

482 surface sediment of Lake Nasser, Egypt. J. Aquat. Res. 40: 213–224.

483 Hakanson, L. 1980. An ecological risk index for aquatic pollution control. A sedimentological

484 approach. Water Res., 14: 975-1001.

485 Huang, K.M., Lin, S. 2003. Consequences and implications of heavy metal spatial variations in

486 sediments of the Keelung River drainage basin, Taiwan. Chemosphere 53: 1113-1121.

487 Kanallopoulos, T.D.; Angelidis, M.O.; Karageorgis, A.P.; Kaberi, H.; Kapsimalis, V.; Anagnostuo,

488 C. 2006. Geochemical composition of the uppermost prodelta sediments of the Evros

489 River, northeastern Aegean Sea. Journal of Marine Systems 63: 63-78.

490 Karageorgis, A. P., Hatzianestis, I. 2003. Surface sediment chemistry in the Olympic Games

491 2004 Sailing Center (SaronikosGulf). Mediterranean Marine Science 4: 5–22.

492 Kumar, A., Yadav, S., Kumar, P., Kumar, R. 2013. Source apportionment and spatial–temporal

493 variations in the metal content of surface dust collected from an industrial area adjoining

494 Delhi, India. Science of the Total Environment 443: 662-672.

495 Lario, J.; Zazo, C.; Goy, J.L.; Dabrio, C.J.; Borja, F.; Silva, P.G.; Sierro, F.; Gonzalez, F.; Soler,

496 V.; Yll, R. 2002. Changes in sedimentation trends in SW Iberia Holocene estuaries.

497 Quaternary International 93-94: 171-176.

18

498   Lario, J.; Zazo, C.; Goy, J.L.; Cabero, A.; Bardaji, T.; Dabrio, C.J.; Borja, F.; Civis, J.; Borja, C.;

499   Spencer, C.; Alonso-Azcarate, J. 2009. Estuarine infill after the last postglacial

500   transgression in Rio Piedras marshland (Gulf of Cádiz, Southern Spain). In: Quaternary

501   Land-Ocean Interactions: Driving mechanisms and coastal responses. IGCP 495 Annual

502   Conference, South Carolina, USA, pp. 56-57.

503   Lario, J., Luque, L., Zazo, C. Goy, J.L., Spencer, C., Cabero, A., Bardají, T., Borja, F., Dabrio,

504   C.J., Civis, J., González-Delgado, J.A., Borja, C., Alonso-Azcárate, J. 2010. Tsunami vs.

505   Storm surge deposits: a review of the sedimentological and geomorphological records of

506   extreme wave events (EWE) during the Holocene in the Gulf of Cadiz, Spain. Z.

507   Geomorph. 54, Suppl.3 301-316.

508   Lario, J., Zazo, C., Goy, J.L., Silva, P.G., Bardají, T., Cabero, A., Dabrio, C.J. 2011. Holocene

509   paleotsunami catalogue of SW Iberia. Quaternary International 242: 196-200.

510   Leblanc, M.; Morales, J.A.; Borrego, J.; Elbaz-Poulichet, F. 2000. 4,500 year-old mining

511   pollution in southwestern Spain: long term implications for modern mining pollution.

512   Econ. Geol. 95: 655-662.

513   Loska, K., Wiechula, D., Barska, B., Cebula, E., Chojnecka, A. 2003. Assessment of Arsenic

514   enrichment of cultivated soils in Southern Poland. Polish Journal of Environmental

515   Studies 2: 187-192.

516   Loska, K., Wiechula, D., Korus, I. 2004. Metal contamination of farming soils affected by

517   industry. Environ. Inter. 30: 159-165.

518   Lozano-Soria, O., Borrego,J., López-González, N., Carro, B. 2005. Características geoquímicas

519   y factores de enriquecimiento (FE) de los sedimentos estuarinos de la Costa de Huelva

520   (SW España). Geogaceta 38: 147-150.

521   Ma, X., Zuo, H., Tian, M., Zhang, L., Meng, J., Zhou, X., Min, N., Chang, X., Liu, Y. 2016.

522   Assessment of heavy metals contamination in sediments from threeadjacent regions of

523   the Yellow River using metal chemical fractions and multivariate analysis techniques.

524   Chemosphere 144: 264-272.

525   Müller, G. 1969. Index of geoaccumulation in sediments of the Rhine River. Geojournal 2: 108-

526   118.

527   Müller, G. 1979. Schwermetalle in den sediments des Rheins-Veranderungen seitt 1971.

528   Umschan 79: 778-783.

529   Müller, G. 1981. The heavy metal pollution of the sediments of Neckars and its tributary: A

530   stocktaking. Chem. Zeit. 105: 157-164.

531   Nocete, F., Álex, E., Nieto, J.M., Sáez, R., Inácio, N., Bayona, M.R. 2005. Intensidad e

532   intensificación en la primera minería y metalurgia del cobre especializada de la

533   Península Ibérica (III milenio ane): la identificación arqueológica de un proceso regional

534   de deforestación y polución. Revista Atlántica-Mediterránea de Prehistoria y Arqueología

535   Social 7: 33-49.

536   Nriagu, J.O., Pacyna, J.M. 1988. Quantitative assessment of worldwide contamination of air,

537   water and soils by trace metals. Nature 333:134-139.

538   Olías, M., Nieto, J.M. 2012. El impacto de la minería en los ríos Tinto y Odiel a lo largo de la

539   historia. Rev. Soc. Geol.España 25:177-192.

540   Pacyna, J.M., Winchester, J.W. 1990. Contamination of the global environment as observed in

541   the Arctic. Palaeogeogr Palaeoclimatol Palaeoecol. 82: 149-57.

542   Palma, P., Ledo, L., Alvarenga, P. 2015. Assessment of trace element pollution and its

543   environmental risk to freshwater sediments influenced by anthropogenic contributions:

544   The case study of Alqueva reservoir (Guadiana Basin). Catena 128: 174-184.

545   Praveena, S.M., Ahmed, A., Radojevic, M., Abdullah, M.H., Aris, A.Z. 2008. Multivariate and

546   Geoaccumulation Index Evaluation in Mangrove Surface Sediment of Mengkabong

547   Lagoon, Sabah. Bull Environ Contam Toxicol. 81: 52-56.

548   Puig, P., Palanques, A., Sánchez-Cabeza, J. A., Masque, P. 1999. Heavy metals in particulate

549   matter and sediments in the southern Barcelona sedimentation system (northwestern

550   Mediterranean). Marine Chemistry, 63: 311-329.

20

551 Quevauviller, P., Lavigne, R., Cortez, L. 1989. Impact of industrial and mine drainage wastes on
552 the heavy metal distribution in the drainage basin and estuary of the Sado River
553 (Portugal). Environ Pollut. 59: 267- 286.

554 Radakovitch, O., Roussiez, V., Ollivier, P., Ludwig,W., Grenz, C., Probst, J. L. 2008. Input of
555 particulate heavy metals from rivers and associated sedimentary deposits on the Gulf of
556 Lion continental shelf. Estuar Coast Shelf Sci. 77: 285-295.

557 Reimann, C., De Caritat, P. 2000. Intrinsic flaws of element enrichment factors (EFs) in
558 environmental geochemistry. Environ. Sci. Technol. 34: 5084-5091.

559 Rivera M.B., Fernández-Caliani, J.C., Giráldez, M.I. 2015. Geoavailability of lithogenic trace
560 elements of environmental concern and supergene enrichment in soils of the Sierra de
561 Aracena Natural Park (SW Spain). Geoderma 259-260:164-173.

562 Rubio, B., Nombela, M.A., Vilas, F. 2000. Geochemistry of major and trace elements in
563 sediments of the Ria de Vigo (NW Spain): an assessment of metal pollution. Mar. Pollut.
564 Bull. 40: 968-980.

565 Ruiz, F., Gonzalez-Regalado, M.L., Borrego, J., Morales, J.A., Pendón, J.G., Muñoz, J.M. 1998.
566 Stratigraphic sequence, elemental concentrations and heavy metal pollution in Holocene
567 sediments from the Tinto-Odiel Estuary, southwestern Spain. Environmental Geology 34:
568 270-278.

569 Ruiz, F. 2001. Trace metals in estuarine sediments from the southwestern Spanish coast. Mar.
570 Pollut. Bull. 42: 481-489.

571 Ruiz, F., Borrego, J., González-Regalado, M.L., López-González, N., Carro, B., Abad, M. 2008.
572 Impact of millennial mining activities on sediments and microfauna of the Tinto River
573 estuary (SW Spain). Marine Pollution Bulletin 56: 1258-1264.

574 Ruiz, F., Borrego, J., González-Regalado, M.L., López-González, N., Carro, B., Abad, M. 2009.
575 Interaction between sedimentary processes, historical pollution and microfauna in the
576 Tinto Estuary (SW Spain). Environmental Geology 58: 779-783.

21

577 Sainz, A., Ruiz, F. 2006. Influence of the very polluted inputs of the Tinto-Odiel system on the
578   adjacent litoral sediments of southwestern Spain: a statistical approach. Chemosphere
579   62: 1612-1622.

580 Santos Bermejo, J.C., Beltrán, R., Gómez Ariza, J.L. 2003. Spatial variations of heavy metals
581   contamination in sediments from Odiel river (Southwest Spain). Environment
582   International 29: 69-77.

583 Schiff, K.C., Weisberg, S. 1999. Iron as a reference element for determining trace metal
584   enrichement in California coastal shelf sediments. Mar Environ Res. 48: 161-179.

585 Schneider, H., Hofer, D., Trog, C., Busch, S., Schneider, M., Baade, J., Daut, G.,
586   Mausbacher, R. 2010. Holocene estuary development in the Algarve Region
587   (Southern Portugal) - a reconstruction of sedimentological and ecological
588   evolution. Quaternary International 221: 141-158.

589 Selvaraj, K., Ram Mohan, V., Szefer, P. 2004. Evaluation of metal contamination in coastal
590   sediments of the Bay of Bengal, India: geochemical and statistical approaches. Mar.
591   Pollut. Bull. 49: 174-185.

592 Sinex, S.A., Helz, G.R. 1981. Regional geochemistry of trace elements in Chesapeake Bay
593   sediments. Environmental Geology 3: 315-323.

594 Srinivasa Reddy, Shaik Basha, Sravan Kumar, V.G., Joshi, H.V., Ramachandraiah, G. 2004.
595   Distribution, enrichment and accumulation of heavy metals in coastal sediments of
596   Alang–Sosiya ship scrapping yard, India. Marine Pollution Bulletin 48: 1055-1059.

597 Soares, H.M.V.M., Boaventura, R.A.R., Machado, A.A.S.C., Da Silva, J.C.G.E. 1999. Sediments
598   as monitors of heavy metal contamination in the Ave river basin (Portugal): multivariate
599   analysis of data. Environ. Poll. 105: 311-323.

600 Sutherland, R.A. 2000. Bed sediments associated trace metals in an urban stream, Oahu,
601   Hawaii. Environ. Geol. 39: 611-627.

602 USEPA. 1996. Microwave Assisted Acid Digestion of Sediments, Sludges, Soils and Oils,
603   Method 3051A. USEPA, Washington, DC, USA.

604   Vazquez, F. G., Sharma, V. K. 2004. Major and trace elements in sediments of the Campeche

605   Sound, southeast Gulf of Mexico. Mar. Poll. Bull. 48: 87-90.

606   Wang, F., Chen, J.: 2000. Relation of sediment characteristics to trace metal concentrations: a

607   statistical study. Wat. Res. 34: 694-698.

608   Woitke, P., Wellmitz, J., Helm, D., Kube, P., Lepom, P., Literaty, P.: 2003. Analysis and

609   assessment of heavy metal pollution in suspended solids and sediments of the river

610   Danube. Chemosphere 51: 633-642.

611   Yaqin, J., Yinchang, F., Jianhui, W., Tan, Z., Zhipeng, B.; Chiqing, D. 2008. Using

612   geoaccumulation index to study source profiles of soil dust in China. Journal of

613   Environmental Sciences 20: 571-578.

614   Zahra, A. Hashmi, M.Z.; Malik, R.N., Ahmed, Z. 2014. Enrichment and geo-accumulation of

615   heavy metals and risk assessment of sediments of the Kurang Nallah-Feeding tributary

616   of the Rawal Lake Reservoir, Pakistan. Science of the Total Environment 470-471: 925-

617   933.

618

619

620   Figures caption:

621   Figure 1. Location of the study area and cores.

622   Figure 2. Geological map of the study area.

623   Figure 3. Sedimentology of the cores and cross section, with indication of the Holocene estuary

624   sequence studied.

Figure1 Click here to download Figure Figure 1.jpg ⬇

Figure2

Figure3

Click here to download Figure Figure 3.jpg
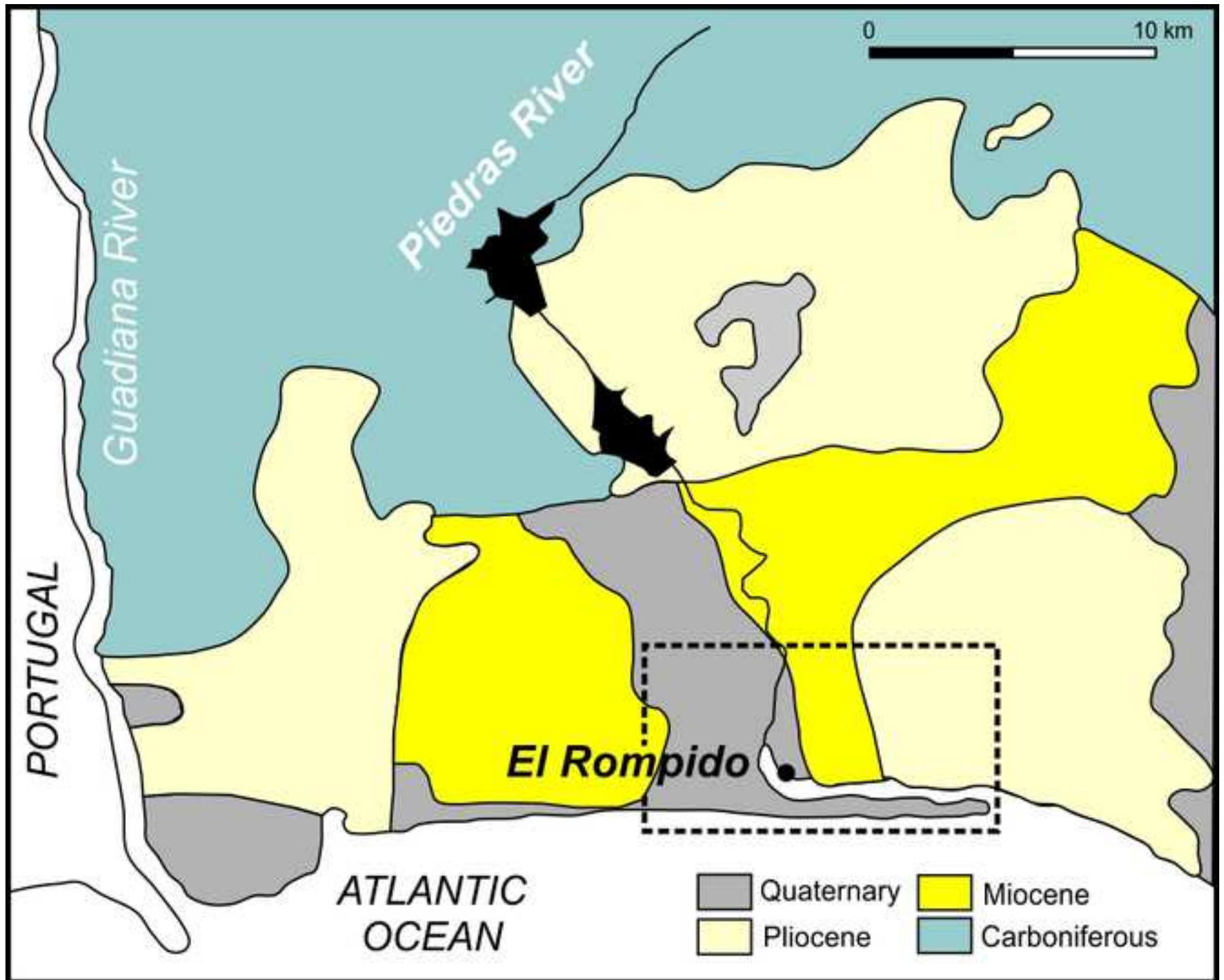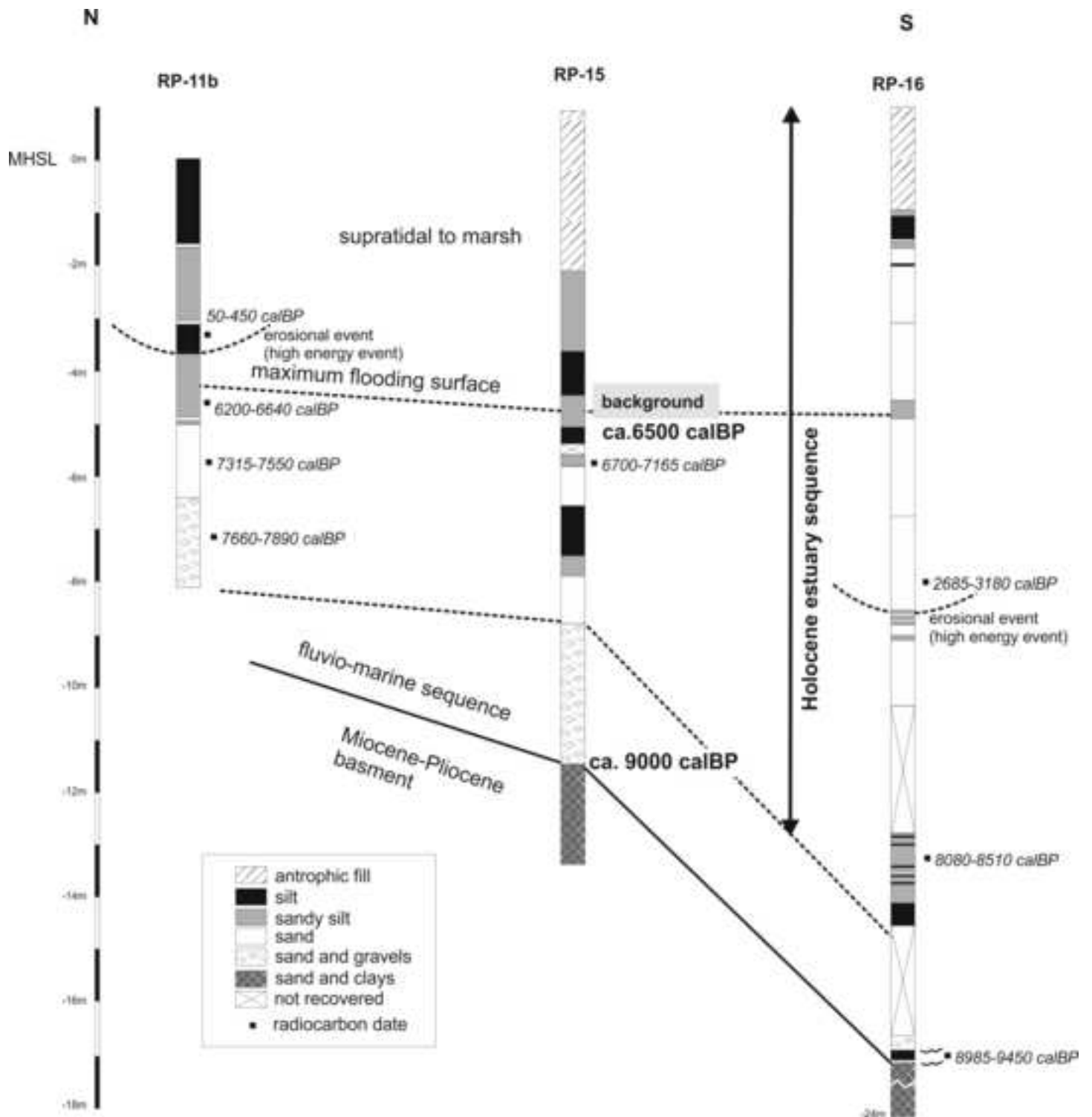
Table1

Table 1. Background geochemical values calculated in the different estuaries of the Southwestern Spanish Coast (element concentrations in mg/Kg).

Estuary	Cr	Cu	Ni	Pb	Zn
Tinto-Odiel[1]	21.1	13.0	12.4	15.4	39.0
Guadiana[2]	23.4	28.0	32.6	19.7	76.4
Doñana[3]	69.6	19.0	27.2	12.6	62.2
Piedras (this work)	45.8	16.1	27.2	13.7	62.2

[1] Ruiz et al., 1998, [2] Delgado et al., 2012, [3] Carretero et al, 2011

Table2

Table 2. Particle size distribution, organic carbon content and metal concentration values in RP-11b core. (mbsl: metres below sea level. Element concentrations in mg/Kg).

mbsl	% Sand	% Silt	% Clay	TOC	Cr	Cu	Ni	Pb	Zn	Al$_2$O$_3$	Fe$_2$O$_3$
0.10	61.06	34.28	4.66	1.49	37.55	19.33	25.8	17.22	69.63	161506	45986
0.29	52.21	40.28	7.51	0.82	45.05	23.72	31.28	27.98	92.05	190818	55534
0.50	16.59	73.33	10.08	1.12	58.95	25.58	31.95	25.39	119.17	189343	44251
0.69	31.22	57.64	11.13	1.7	49.99	21.34	27.6	8.24	52.76	170146	42832
0.89	22.42	69.89	7.69	1.53	47.97	17.19	31.3	13.59	67.83	192775	53833
1.09	29.86	64.13	6.02	1.66	55.24	17.38	31.85	13.96	73.55	192871	50667
1.28	36.21	58.53	5.26	1.66	53.92	18.64	31.18	18.35	66.65	184790	52880
1.49	31.22	56.92	11.86	1.29	55.62	18.00	30.81	15.24	68.61	197444	49894
1.65	25.27	66.33	8.39	1.31	52.74	20.23	32.47	15.9	72.75	189187	63720
1.89	34.78	58.19	7.04	1.17	45.84	19.15	29.8	21.22	73.14	182385	52251
2.09	47.62	46.99	5.39	1.53	61.09	20.38	34.16	18.90	79.98	192762	53319
2.29	14.75	76.77	8.48	1.20	51.42	19.65	30.19	16.09	72.53	197418	52888
2.49	34.19	61.20	4.61	1.70	54.32	17.12	29.17	13.21	65.54	185522	52702
2.69	28.04	71.96	0.00	1.45	50.06	20.03	30.75	15.10	71.53	188733	50499
2.89	37.42	56.20	6.38	0.97	50.82	18.17	29.47	13.64	65.56	188246	49440
3.09	53.18	41.79	5.03	0.87	44.63	17.13	28.52	14.33	60.86	165662	44644
3.29	35.18	57.45	7.37	1.43	48.55	20.71	35.11	20.54	69.98	182468	53106
3.49	35.53	57.33	7.14	1.64	45.11	17.33	29.71	14.68	68.36	186184	54879
3.69	54.64	40.73	4.63	1.76	43.97	17.63	28.65	14.54	69.07	177240	52858
3.89	30.46	61.78	7.76	1.29	53.24	19.23	31.24	15.44	67.21	189073	50774
4.09	30.97	61.92	7.11	1.03	53.73	19.35	32.65	15.41	68.52	187531	49340
4.29	27.62	65.11	7.26	1.22	54.17	18.37	30.41	14.30	66.86	155523	48899
4.49	54.45	41.05	4.50	1.11	55.17	16.54	30.09	14.85	59.87	188105	50943
4.69	52.72	42.08	5.20	0.99	51.04	17.63	30.66	14.23	65.84	182065	45736
4.89	49.88	45.68	4.45	1.09	57.62	17.69	32.44	15.61	63.00	186608	64058
5.09	28.97	60.86	10.17	0.60	55.87	17.16	31.77	15.63	60.99	162571	48540
5.28	77.37	19.32	3.31	0.12	45.57	16.15	25.16	14.00	51.43	98949	22145
5.48	71.53	23.81	4.66	0.08	39.44	12.99	23.6	11.30	47.00	76949	15868
5.60	74.58	20.94	4.49	0.04	37.61	15.09	21.28	11.98	46.39	88591	17805
5.79	87.54	9.76	2.70	0.02	30.74	9.44	18.38	8.48	37.59	73571	14587
6.00	91.45	6.91	1.63	0.03	34.52	10.67	20.23	9.34	43.96	86234	15905
6.20	87.03	11.33	1.63	0.16	33.44	13.58	26.49	10.41	43.53	95478	21936

Table3

Table 3. Particle size distribution, organic carbon content and metal concentration values in RP-15 core. (mbsl: metres below sea level. Element concentrations in mg/Kg)

mbsl	% Sand	% Silt	% Clay	TOC	Cr	Cu	Ni	Pb	Zn	Al$_2$O$_3$	Fe$_2$O$_3$
3.70	32.90	60.19	6.91	1.09	47.67	15.93	27.22	13.77	66.81	177806	50918
3.89	34.81	58.16	7.03	0.98	51.04	15.22	28.25	14.76	65.69	176185	40688
4.09	35.25	58.00	6.74	1.01	45.06	13.94	26.15	13.36	57.04	173337	44966
4.29	29.56	61.20	9.24	1.19	47.50	18.02	29.35	14.17	66.47	169573	58714
4.54	42.19	51.29	6.52	1.02	53.18	17.36	30.2	15.34	67.16	159252	47971
4.69	39.50	53.39	7.11	0.98	41.57	15.69	26.09	14.87	68.04	170923	45714
4.93	21.61	68.64	9.75	0.95	40.10	16.06	26.65	13.47	57.52	168593	50820
5.09	22.77	69.06	8.17	0.98	47.77	16.04	28.19	13.2	61.69	183076	52808
5.29	24.89	67.44	7.67	1.05	44.01	15.04	26.11	12.98	62.59	175093	48227
5.49	20.91	71.72	7.37	0.91	41.88	15.54	25.94	13.17	57.59	169596	49042
5.69	16.14	75.07	8.79	0.99	40.05	12.81	23.51	12.50	52.15	164926	50526
5.90	33.59	59.32	7.09	1.03	47.49	16.66	27.30	14.20	67.06	167941	44818
6.01	36.15	56.71	7.14	0.89	44.63	14.60	24.00	13.59	60.00	160834	47010
6.13	23.07	68.50	8.43	0.93	48.82	16.38	28.73	13.64	64.35	169989	50802
6.30	30.80	61.67	7.54	0.88	49.92	18.79	29.52	15.24	83.20	170026	55116
6.52	16.01	74.46	9.53	0.89	42.52	14.64	24.51	12.62	58.74	171648	51189
6.70	26.62	64.60	8.78	0.74	38.72	13.17	24.38	13.58	56.00	173312	46727
6.90	40.67	52.13	7.20	0.33	36.99	11.76	21.63	10.03	39.39	126078	38015
7.12	24.98	66.60	8.42	0.95	47.57	14.29	26.49	13.11	59.00	171095	54587
7.31	39.23	54.50	6.27	0.99	40.50	14.27	23.79	14.02	53.06	159653	45600
7.50	46.96	46.20	6.84	0.27	31.95	10.54	19.07	10.48	36.86	156843	43523
7.71	40.14	51.52	8.35	0.34	38.61	11.35	20.38	10.67	40.39	133480	37751
7.90	21.36	71.99	6.65	0.43	40.49	13.80	22.30	11.56	47.33	161497	48223
8.09	28.73	63.61	7.67	0.47	42.56	13.21	23.18	12.97	45.45	170303	47636
8.10	44.10	48.39	7.51	0.36	31.21	10.33	18.00	9.94	35.04	150686	40266
8.33	23.36	68.29	8.35	0.87	42.47	15.05	25.59	15.11	53.33	171038	50165
8.49	42.61	49.26	8.13	0.80	47.28	13.51	24.97	11.41	50.17	155540	46329
8.70	14.98	73.67	11.35	0.50	46.40	13.50	24.83	13.4	49.47	161646	45009
8.99	23.68	66.18	10.14	0.99	52.88	14.87	32.00	16.7	61.82	189026	56261
9.10	28.57	61.44	10.00	1.00	58.73	15.09	32.45	16.24	65.15	192972	57210
9.20	30.10	61.10	8.80	1.30	58.30	18.94	36.64	19.29	67.80	176538	55499
9.30	30.09	59.39	10.52	1.39	46.38	18.31	33.62	20.09	58.82	183334	51873
9.45	69.16	24.61	6.22	0.19	36.97	18.18	25.34	13.95	51.98	72673	16965
9.50	76.21	18.72	5.07	0.10	38.21	20.73	25.65	13.40	49.22	72336	16364
9.63	19.35	69.39	11.26	0.65	41.97	13.14	24.17	12.21	48.38	159643	44688
9.79	71.19	23.64	5.16	0.03	31.54	18.82	21.75	14.13	39.95	84269	17435
9.99	75.55	20.03	4.42	0.05	31.2	18.27	21.44	11.68	37.21	86544	17376
10.20	86.12	10.11	3.77	0.00	29.04	14.88	18.29	9.25	34.30	65305	16533
10.40	74.29	21.03	4.68	0.12	34.48	31.46	22.48	10.86	49.77	83895	18248
10.59	92.69	5.23	2.09	0.06	31.45	20.59	20.10	11.44	39.13	99053	22223

Table4

Table 4. Particle size distribution, organic carbon content and metal concentration values in RP-16 core. (mbsl: metres below sea level. Element concentrations in mg/kg).

mbsl	% Sand	% Silt	% Clay	TOC	Cr	Cu	Ni	Pb	Zn	Al_2O_3	Fe_2O_3
2.10	55.44	36.38	8.18	0.65	58.58	23.00	32.68	28.49	85.21	182912	70283
2.29	51.62	40.46	7.92	0.65	57.17	23.11	31.57	30.74	79.57	165893	51757
2.50	79.45	16.93	3.62	0.6	53.33	22.8	29.83	31.03	77.07	136998	40936
2.62	88.84	9.29	1.87	0.54	56.03	25.67	30.12	26.45	78.34	146078	34965
5.80	90.91	7.39	1.70	0.21	35.33	10.14	19.89	18.73	49.82	79822	16007
8.70	95.66	3.42	0.92	0.00	23.51	22.62	11.86	13.4	39.48	37798	8203
8.95	91.41	6.52	2.07	0.00	13.25	5.31	6.14	6.38	18.51	30830	6296
9.85	88.52	9.35	2.14	0.15	25.15	8.64	13.54	6.36	31.68	46870	11090
10.00	90.95	6.85	2.20	0.00	14.06	14.53	6.78	3.76	22.94	25911	7121
10.55	87.78	9.63	2.59	0.03	11.50	5.55	7.49	4.18	15.37	23871	5142
11.15	90.17	8.06	1.77	0.00	13.30	9.71	6.60	4.24	19.54	27007	5770
13.85	77.63	18.06	4.31	0.20	48.62	16.00	26.97	14.16	60.33	111122	33577
14.05	81.63	15.17	3.20	0.30	51.11	14.58	27.48	13.95	56.71	115433	37485
14.71	80.20	15.73	4.07	0.32	36.47	14.05	24.91	14.03	51.11	107349	32098
14.89	93.63	4.94	1.43	0.19	51.29	14.34	25.38	11.99	52.25	79556	23856
15.18	58.71	35.27	6.02	0.23	48.29	13.63	24.86	12.67	51.60	90230	25169
15.39	20.62	70.60	8.77	0.42	46.99	15.23	29.09	14.43	58.61	166767	53537
15.54	70.27	25.18	4.55	0.71	36.56	13.24	23.66	12.36	48.99	143289	38801
18.04	22.60	67.95	9.45	0.72	48.7	15.31	29.81	15.21	66.57	177508	56209

Table5

Table 5. Metal concentration in selected time slices (element concentrations in mg/Kg. Bold numbers indicated values used to calculate the backround).

Age	Cr	Cu	Ni	Pb	Zn	Al_2O_3	Fe_2O_3 total
Core RP-15							
ca.4000 calBP	47.96	14.57	27.18	14.04	61.21	174755	42774
ca.6500 calBP	**43.42**	**14.87**	**25.14**	**13.35**	**58.96**	**165791**	**47801**
ca.7000 calBP	35.97	12.06	20.62	11.01	41.77	159153	45812
ca. 7500 calBP	44.88	14.28	25.28	13.26	51.75	163289	48247
8000-8500 calBP	44.97	19.04	30.31	16.68	59.96	126220	35175
ca. 9000 calBP	31.45	20.59	20.10	11.44	39.13	99053	22223
Core RP-11b							
surface	41.30	21.53	28.54	22.60	80.84	176162	50760
ca. 250 calBP	46.10	18.39	31.11	16.52	66.40	178104	50876
ca. 6500 calBP	54.93	17.26	31.24	15.08	62.43	179837	52319
ca. 7500 calBP	34.92	10.67	20.23	9.34	43.96	86234	15905
Core RP-16							
surface (1 m)	58.58	23.00	32.68	28.49	85.21	182912	70283
ca. 3000 calBP	13.25	5.31	6.14	6.38	18.51	30830	6296
ca. 8000-8500 calBP	46.29	14.32	29.52	13.32	53.36	100779	31146
ca. 9000 calBP	48.70	15.31	29.81	15.21	66.57	177508	56209

Table6

Table 6. Contamination Factor (CF) and Contamination Degree (CD) in the selected time slices

Age	Cr	Cu	Ni	Pb	Zn	CD
Core RP-15						
ca.4000 calBP	1.10	0.98	1.08	1.05	1.04	5.25
ca.6500 calBP			background			
ca.7000 calBP	0.83	0.81	0.82	0.82	0.71	3.99
ca. 7500 calBP	1.03	0.96	1.01	0.99	0.88	4.87
8000-8500 calBP	1.04	1.28	1.21	1.25	0.97	5.75
ca. 9000 calBP	0.72	1.39	0.80	0.86	0.66	4.43
Core RP-11b						
surface	0.95	1.45	1.14	1.69	1.37	6.60
ca. 250 calBP	1.06	1.24	1.24	1.24	1.13	5.91
ca. 6500 calBP	1.26	1.16	1.24	1.13	1.06	5.85
ca. 7500 calBP	0.80	0.72	0.80	0.70	0.75	3.77
Core RP-16						
surface (1 m)	1.35	1.55	1.30	2.13	1.45	7.78
ca. 3000 calBP	0.31	0.36	0.24	0.48	0.31	1.70
ca. 8000-8500 calBP	1.07	0.97	1.03	1.00	0.90	4.97
ca. 9000 calBP	1.05	0.96	1.11	0.11	1.05	4.28

Table7

Table 7. Geoaccumulation Index (I_{geo})in the selected time slices

Age	I_{geo}				
	Cr	Cu	Ni	Pb	Zn
Core RP-15					
ca.4000 calBP	-0.41	-0.48	-0.68	-0.73	-0.75
ca.6500 calBP	background				
ca.7000 calBP	-0.82	-0.91	-0.88	-0.88	-1.10
ca. 7500 calBP	-0.54	-0.64	-0.58	-0.61	-0.77
8000-8500 calBP	-0.56	-0.23	-0.33	-0.29	-0.65
ca. 9000 calBP	-1.05	-0.11	-0.91	-0.81	-1.18
Core RP-11b					
surface	-0.66	-0.06	-0.41	0.13	-0.14
ca. 250 calBP	-0.50	-0.28	-0.28	-0.30	-0.42
ca. 6500 calBP	-0.25	-0.37	-0.27	-0.41	-0.50
ca. 7500 calBP	-0.92	-1.06	-0.90	-1.10	-1.01
Core RP-16					
surface (1 m)	-0.15	0.05	-0.21	0.51	-0.05
ca. 3000 calBP	-2.30	-2.07	-2.62	-1.65	-2.26
ca. 8000-8500 calBP	-0.51	0.64	-0.54	-0.59	-0.73
ca. 9000 calBP	-0.42	-0.54	-0.34	-0.40	-0.41

Table8

Table 8. Enrichment Factors (Al and Fe) in the selected time slices

Age	EF$_{Al}$					EF$_{Fe}$				
	Cr	**Cu**	**Ni**	**Pb**	**Zn**	**Cr**	**Cu**	**Ni**	**Pb**	**Zn**
Core RP-15										
ca.4000 calBP	1.05	0.93	1.03	0.10	0.99	1.23	1.10	1.21	1.18	1.16
ca.6500 calBP					**background**					
ca.7000 calBP	0.87	0.85	0.85	0.09	0.74	0.86	0.85	0.86	0.86	0.74
ca. 7500 calBP	1.06	0.98	1.02	0.10	0.89	1.03	0.95	1.00	0.98	0.87
8000-8500 calBP	1.55	2.08	1.80	0.19	1.48	1.78	2.44	2.08	2.13	1.71
ca. 9000 calBP	1.22	2.32	1.34	0.14	1.11	1.56	2.99	1.72	1.84	1.43
Core RP-11b										
surface	0.90	1.36	1.07	0.16	1.28	0.90	1.37	1.07	1.57	1.29
ca. 250 calBP	0.99	1.15	1.15	0.12	1.05	1.00	1.17	1.17	1.16	1.06
ca. 6500 calBP	1.17	1.08	1.15	0.10	0.98	1.17	1.08	1.15	1.05	0.98
ca. 7500 calBP	1.53	1.38	1.55	0.13	1.43	2.39	2.16	2.42	2.10	2.24
Core RP-16										
surface (1 m)	1.23	1.40	1.18	0.19	1.31	0.92	1.05	0.88	1.45	0.98
ca. 3000 calBP	1.65	1.92	1.31	0.26	1.69	2.32	2.72	1.85	3.63	2.38
ca. 8000-8500 calBP	1.82	1.63	1.74	0.17	1.52	1.71	1.53	1.63	1.57	1.43
ca. 9000 calBP	1.05	0.96	1.11	0.11	1.05	0.95	0.88	1.01	0.97	0.96

Table9

Table 9. Pearson correlation matrix showing the coefficients of correlation among grain size fractions. TOC and heavy metal contents in the RP-15 core. n=40

	Sand	Silt	Clay	TOC	Cr	Cu	Ni	Pb	Zn
Sand	1								
Silt	-0.998	1							
Clay	-0.850	0.820	1						
TOC	-0.744	0.744	0.613	1					
Cr	-0.618	0.612	0.577	0.801	1				
Cu	0.486	-0.486	-0.405	-0.149	-0.022	1			
Ni	-0.452	0.439	0.501	0.777	0.889	0.228	1		
Pb	-0.341	0.327	0.418	0.680	0.709	0.219	0.897	1	
Zn	-0.517	0.523	0.382	0.808	0.818	0.197	0.820	0.685	1

Table10

Table 10. Pearson correlation matrix showing the coefficients of correlation among grain size fractions. TOC and heavy metal contents in the RP-11b core. n=32

	Sand	Silt	Clay	TOC	Cr	Cu	Ni	Pb	Zn
Sand	1								
Silt	-0.995	1							
Clay	-0.682	0.604	1						
TOC	-0.744	0.758	0.381	1					
Cr	-0.770	0.767	0.519	0.605	1				
Cu	-0.728	0.715	0.568	0.625	0.639	1			
Ni	-0.785	0.788	0.485	0.698	0.830	0.752	1		
Pb	-0.418	0.409	0.337	0.309	0.409	0.766	0.600	1	
Zn	-0.665	0.660	0.464	0.543	0.604	0.864	0.685	0.850	1

Table11

Table 11. Pearson correlation matrix showing the coefficients of correlation among grain size fractions. TOC and heavy metal contents in the RP16 stratigraphic cross section. n=19

	Sand	Silt	Clay	TOC	Cr	Cu	Ni	Pb	Zn
Sand	1								
Silt	-0.999	1							
Clay	-0.961	0.950	1						
TOC	-0.643	0.632	0.697	1					
Cr	-0.498	0.488	0.556	0.764	1				
Cu	-0.225	0.215	0.289	0.576	0.690	1			
Ni	-0.587	0.576	0.638	0.836	0.978	0.655	1		
Pb	-0.312	0.297	0.413	0.750	0.807	0.816	0.794	1	
Zn	-0.498	0.484	0.575	0.837	0.954	0.809	0.954	0.920	1